EURASIAN JOURNAL OF MATHEMATICAL AND COMPUTER APPLICATIONS
ISSN 2077–9879
Volume 1, Number 1 (2013) 103 – 124

STREAMLINE-BASED SIMULATION OF 2-D 2-PHASE OIL DISPLACEMENT BY POLYMER SLUGS

Bruno J. Vicente, Viatcheslav I. Priimenko, and Adolfo P. Pires

Abstract The injection of polymers is a widespread Enhanced Oil Recovery (EOR) technique. However, the continuous injection may be very expensive, and the slug (discontinuous) injection is an alternative to improve the recovery factor. In this paper, streamline simulation is used to model the 2-D 2-phase oil displacement by polymer slugs, considering adsorption effects characterized by the Henry and Langmuir isotherms. Streamline simulation can be much faster than conventional finite difference models and its results may be used for slug polymer injection evaluation in heterogeneous reservoirs. It decouples the 2-D problem into multiple 1-D problems along streamlines. The mass transport equations in the streamlines are solved implicitly, through the method of characteristics. The continuous polymer injection is a Riemann problem and its solution is self-similar, but in the case of slug injection, there are interactions between waves of different families. In this work we extend the streamline-based technique to the case of slug injection, incorporating the implicit-form solutions of the corresponding transport problems into the numerical process. Such solutions are free from numerical diffusion, and allow the use of bigger time steps. The simulations were run in 2-D incompressible models without gravity effects. Results obtained were compared to a finite-difference simulation. The solutions along streamlines allowed the exact modeling of shock and rarefaction waves as well as the interaction between waves of same and different families.

Key words: Porous media, 2-D hyperbolic model, streamline simulation, implicit-form solutions, saturation and concentration maps

AMS Mathematics Subject Classification: Primary: 76T99; Secondary: 35Q35, 65M06

1 Introduction

Waterflooding is the most widely used method of secondary oil recovery by petroleum industry. This technique became more important in the 50's, when their main weaknesses and strengths were also identified. Waterflooding at unfavorable mobility ratio or in strongly heterogeneous reservoirs does not show satisfactory results. Polymer flooding is an alternative to improve oil recovery in such scenarios [1, 2]. The polymer increases the aqueous-phase viscosity and may, in addition, decrease the effective permeability to it. Thus, the area swept by water is increased and water breakthrough is delayed. The main drawback of a polymer injection project is the price of the polymer; and it may be overcome through the use of a polymer slug driven by water.

A fast and robust full field scale simulator that includes a polymer flooding option is of fundamental importance for preliminary evaluation of different secondary and improved oil recovery options for a given reservoir. During the simulation of slug polymer flooding, an important issue to be considered is the adsorption of the chemical component in porous media. Depending on the adsorption isotherm different zones with varying concentration of polymer both ahead and behind of the slug may appear. Since certain polymer solution properties depend on concentration, e.g., the viscosity, simulation models should take this effect into account.

Traditionally, such simulations are performed through finite differences based numerical models, well suited to represent the complex physics of the problem, but these models lead to results with numerical diffusion. Streamline simulation is an alternative to overcome the limitations presented by conventional simulators. This technique is based on an analogy between streamlines and seismic ray tracing, and permits to reduce multidimensional transport equations into a series of 1-D equations along streamlines, see, e.g., [3].

The streamline approach for modeling multidimensional, multiphase flow basically can be comprised of the following steps:

- tracing streamlines based on an underlying velocity (and consequently, pressure) field using the time-of-flight algorithm as outlined by Datta-Gupta and King in [4],
- computing tracer travel time or time-of-flight along streamlines,
- decoupling the transport equations (concentration and saturation equations) using a coordinate transformation from physical space to the time-of-flight coordinates following flow directions,
- solving (analytically or numerically) the transport equations along streamlines,
- and occasionally updating the streamlines to account for mobility effects or changing field conditions.

The computational advantage of the streamline approach can be attributed to the fact that streamlines do not need to be updated frequently and the transport equations along streamlines are decoupled from the underlying grid, thus allowing for faster solution. The details of streamline simulation can be found in, e.g., [5].

Around 30 years ago, Lake et al. [6] introduced a hybrid streamline approach to model large-scale micellar-polymer flooding combining an areal streamtube model with a cross-sectional finite-difference simulator. Batycky et al. [7] presented a new streamline simulator applicable to field scale flow. The proposed method is three dimensional and accounts for changing well conditions, heterogeneity, mobility effects, and gravity effects. The changing in the mobility field is accounted for when updating the streamline, and in this work the transport equation was solved numerically. Thiele et al. [8] extended this approach to field scale polymer flooding. Clemens et al. [9] used streamline simulation to efficiently manage a field polymer injection project. A new metric was introduced: polymer injection efficiency as a function of time for each

pattern. AlSofi et al. [10, 11] analyzed the performance of polymer flooding considering both Newtonian and non-Newtonian behavior using streamlines simulation.

Fayers and Perrine [12] were among the first to analyze solutions of hyperbolic systems modeling *continuous* polymer injection. Exact analytical solutions were obtained for continuous chemical flooding with one dissolved component [13], with two dissolved components [14] and with any arbitrary number of components [15]. Bedrikovetsky [16] described the hydrodynamics of oil displacement by injection of polymer slugs for different adsorption isotherms.

In this work we extend the streamline-based technique to the case of *discontinuous* polymer injection, incorporating the implicit-form solutions of the corresponding transport problems into numerical process.

The organization of this paper is as follows. First, we formulate a mathematical model describing the displacement of oil by a polymer slug driven by water. Second, the solution of the formulated problem is done considering adsorption effects, described by the Henry and Langmuir isotherms. Next, we formulate the basic steps of the proposed algorithm for the 2-D case. Finally, the validation of the approach and 2-D examples are shown to illustrate the capacity of the proposed method.

2 Mathematical Model Description

The mathematical model is a simplified water/oil two-phase flow in porous media with the following assumptions:

- the flow obeys Darcy's law,
- incompressible flow,
- gravity/capillary effects neglected,
- components diffusion and dispersion are negligible,
- water density does not depend on polymer concentration,
- polymer adsorbs at thermodynamics equilibrium and its adsorption is a function of its concentration in aqueous phase,
- local instantaneous equilibrium exists everywhere.

General Equations

Following the model assumptions, the pressure equation is given by

$$\nabla \cdot [(\lambda_o + \lambda_w)\mathbf{K} \cdot \nabla P] = Q\,, \tag{2.1}$$

where $\mathbf{K}$ is the permeability tensor, Q a source or sink volumetric flow rate, $\lambda_o = k_{ro}\mu_o^{-1}$ and $\lambda_w = k_{rw}\mu_w^{-1}$ are the oil and water mobility respectively, k_{ri} and μ_i are the relative permeability and viscosity of the corresponding phase $i = o, w$.

The transport process is described by the following quasi-linear equations:

$$\begin{aligned} \phi\frac{\partial s}{\partial t} + \mathbf{u}\cdot\nabla f = 0\,, \\ \phi\frac{\partial (cs+a)}{\partial t} + \mathbf{u}\cdot\nabla (cf) = 0\,, \end{aligned} \tag{2.2}$$

where $\mathbf{u}(\mathbf{x})$ is the total velocity, $s(\mathbf{x},t)$ is the water saturation, $c(\mathbf{x},t)$ is the polymer concentration in the water phase, and $(\mathbf{x},t) \in R^3 \times R^+$. The adsorbed concentration is given by $a(c)$, ϕ is the porosity of porous media, and the water fractional flow is defined by

$$f(s,c) = \lambda_w(\lambda_o + \lambda_w)^{-1}\,.$$

The total velocity is calculated using Darcy's law:

$$\mathbf{u} = -(\lambda_o + \lambda_w)\mathbf{K}\nabla\cdot P\,.$$

Coordinate Transformation

The basis for any streamline simulation method is a sequential splitting of the coupled pressure and transport equations. The pressure and velocity are then used as parameters while advancing the transport equations a given time step. Finally, the new field is used as input parameter for a new pressure solution step, and so on.

In reservoir simulation, the most important streamline parameter τ is called time-of-flight, since it can be interpreted as the travel time of a neutral particle along streamline l [5]:

$$\tau = \int_l \frac{\phi}{|\mathbf{u}|} d\zeta\,.$$

Together with the bi-stream functions ψ and χ, for which $\mathbf{u} = \nabla\psi \times \nabla\chi$, the time-of-flight τ form an alternative set of coordinates for 3-D space. The Jacobian of the transformation from physical coordinates to time-of-flight coordinates (τ,ψ,χ) is equal to ϕ . From this, and the fact that $\mathbf{u}$ is orthogonal to $\nabla\psi$ and $\nabla\chi$, it is possible to simplify the directional gradient along $\mathbf{u}$ as follows

$$\mathbf{u}\cdot\nabla = \phi\frac{\partial}{\partial\tau}\,.$$

This operator identity is a key point in any streamline method, allowing multidimensional transport equations (2.2) to be transformed to a family of 1-D transport equations

$$\begin{aligned} \frac{\partial s}{\partial t} + \frac{\partial f}{\partial \tau} = 0\,, \\ \frac{\partial (cs+a)}{\partial t} + \frac{\partial (cf)}{\partial \tau} = 0\,, \end{aligned} \tag{2.3}$$

where the functions $s(\tau,t)$ and $c(\tau,t)$ characterize the 1-D flow along streamlines.

Statement of the Problem

We consider one of the possible mathematical models, widely used in the reservoir characterization, describing the displacement of oil by a polymer slug driven by water. The problem consists in the definition of the concentration c and saturation s satisfying (2.3) and the following initial and boundary conditions:

$$t = 0 : \begin{cases} s = s_I \\ c = 0 \end{cases} \quad \text{and } \tau = 0 : \begin{cases} f = 1 \\ c = \begin{cases} c_J, 0 < t < t_J \,, \\ 0, t > t_J \end{cases} \end{cases} \tag{2.4}$$

where s_I is the initial water saturation, c_J is the concentration of injected polymer and t_J is the injection time.

3 Solution of the Problem

The solution of (2.3)-(2.4) is presented and discussed in details in many books, see, e.g., [17]. We do not present a detailed derivation of the solution, our main goal is the development of the streamlines simulator using the implicit-form solution along streamlines. Such problem is solved by the method of characteristics, and may present two kinds of rarefaction waves [18]:

- s-wave - constant concentration and varying saturation,
- c-wave - varying concentration and saturation.

The hyperbolic system (2.3) also admits shock waves, satisfying the following Rankine-Hugoniot condition:

$$V(t) = \frac{f^+}{s^+ + [a][c]^{-1}} = \frac{f^-}{s^- + [a][c]^{-1}} \,,$$

where $[A] = A^+ - A^-$, and A^- and A^+ are the limiting values from the left $(-)$ and right $(+)$ at the point $(t, \tau_0(t))$ along any discontinuity curve $\tau_0(t)$, and V is the shock speed. In the case of continuous injection the solution is self-similar, i.e.,

$$s = s(\xi) \,, c = c(\xi) \,, \xi = \frac{\tau}{t} \,.$$

In the case of discontinuous (slug) injection the solution is not so trivial because of interactions between waves of different families. In the rarefaction zones the solution is done in the implicit form only. The details of the solution construction are given, e.g., in [18].

Case 1. Linear adsorption isotherm

The linear adsorption isotherm may be represented by Henry's law:

$$a(c) = \Gamma c \,,$$

Region	Concentration	Saturation	Description
I.	$c(\tau,t)=0$	$s(\tau,t)=s_I$	Zone of displaced oil.
II.	$c(\tau,t)=0$	$s_0 < s(\tau,t) < s_1$	The corresponding path in (s,f) plane is represented by part of a curve $f(s,0)$.
III.	$c(\tau,t)=0$	$s(\tau,t)=s_2$	Oil bank.
IV.	$c(\tau,t)=c_J$	$s^+(\tau_0) < s(\tau,t) < s_2$	Polymer slug. The corresponding path in (s,f) plane is represented by part of a curve $f(s,c_J)$.
V.	$c(\tau,t)=0$	$s_J < s(\tau,t) < s^-(\tau_0)$	Water-drive zone. The corresponding path in (s,f) plane is represented by part of a curve $f(s,0)$.

Table 1: Structure of the 1-D problem, case 1

where Γ is the Henry law constant. In this case the jump of concentration is defined by the discontinuity of c at the point $(0,t_J)$, see (2.4). There is an interaction of the jump of concentration with the s-wave of the self-similar solution for $t > t_J$. The path of the discontinuity $\tau_0(t)$ is built using the following system of transcendental equations:

$$\frac{t_J}{t} = \triangle(s^+(\tau_0), c_J))\,, \quad \frac{t_J}{\tau_0(t)} = \frac{\triangle(s^+(\tau_0), c_J))}{f_s'(s^+(\tau_0), c_J)}\,, \tag{3.1}$$

where $\triangle(s,c) = f(s,c) - (s+b)f_s'(s,c)$, $b = [a][c]^{-1}$. Fig.1 presents the solution for this case. The structure of the solution can be divided into four regions, see Table 1 for details. Velocities $V_k, k = 0,1,2$, are calculated through the following expressions:

$$V_0 = \frac{f(s_0,0)}{s_0 - s_I}\,, \; V_1 = f_s'(s_1,0)\,,$$
$$V_2 = f_s'(s_2,c_J) = \frac{f(s_1,0)}{s_1 + [a][c]^{-1}} = \frac{f(s_2,c_J)}{s_2 + [a][c]^{-1}}\,.$$

Case 2. Convex adsorption isotherm

The convex adsorption isotherm ($a''(c) < 0$) can be represented by Langmuir's law:

$$a(c) = \frac{\Gamma_1 c}{1 + \Gamma_2 c}\,,$$

where Γ_n, $n = 1,2$, are the Langmuir constants. In this case, the discontinuity at $(0,t_J)$ produces a c-wave that will interact with a s-wave of the self-similar solution. The discontinuity $\tau_0(t)$ is described by (3.1) with $b = a'(c_J)$. For $t > t_1$ (Fig.2b) the trajectory of the front of polymer slug t_1 satisfies the following transcendental equations:

$$\frac{d\tau_1}{dt} = \frac{f(s^-(\tau_1), c^-(\tau_1))}{s^-(\tau_1) + [a][c]^{-1}} = \frac{f(s^+(\tau_1),0)}{s^+(\tau_1) + [a][c]^{-1}} = f_s'(s^-(\tau_1), c^-(\tau_1))\,,$$
$$\tau_1(t)[a(c^-(\tau_1)) - a'(c^-(\tau_1))c^-(\tau_1)] = c_J\,.$$

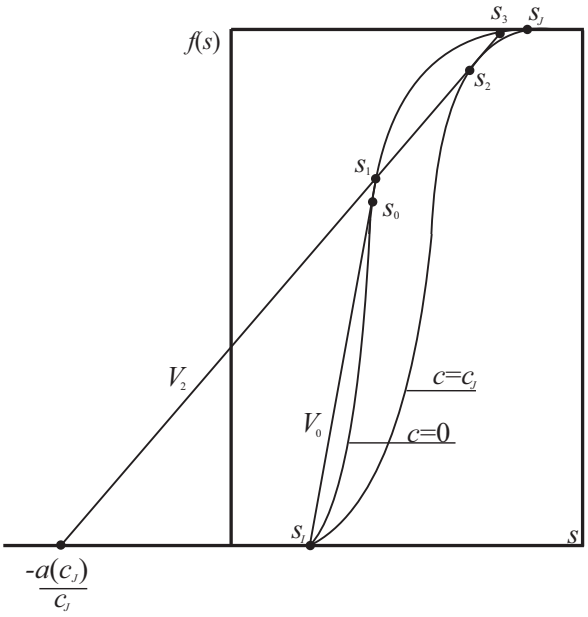

(a) (s, f)-plane

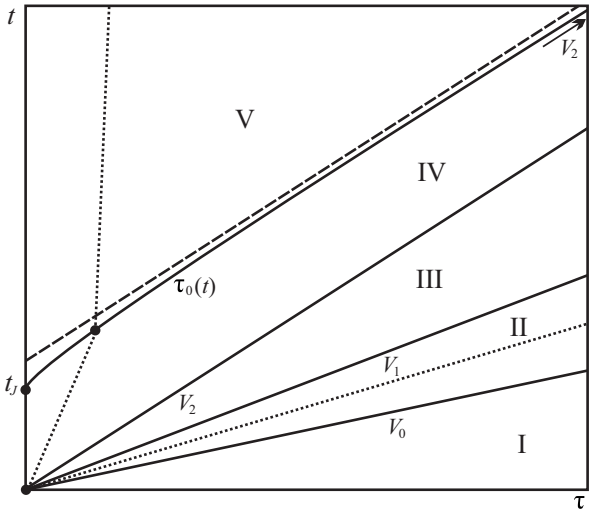

(b) (τ, t)- plane

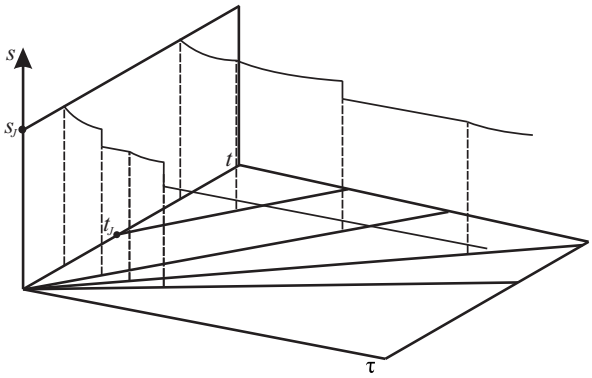

(c) Saturation - $s(\tau, t)$

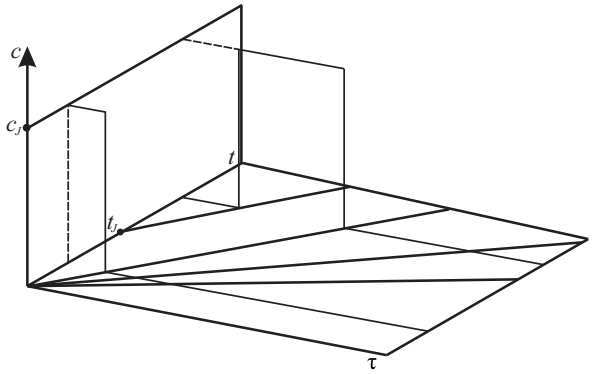

(d) Concentration - $c(\tau, t)$

Figure 1: Solution of the 1-D problem, case 1

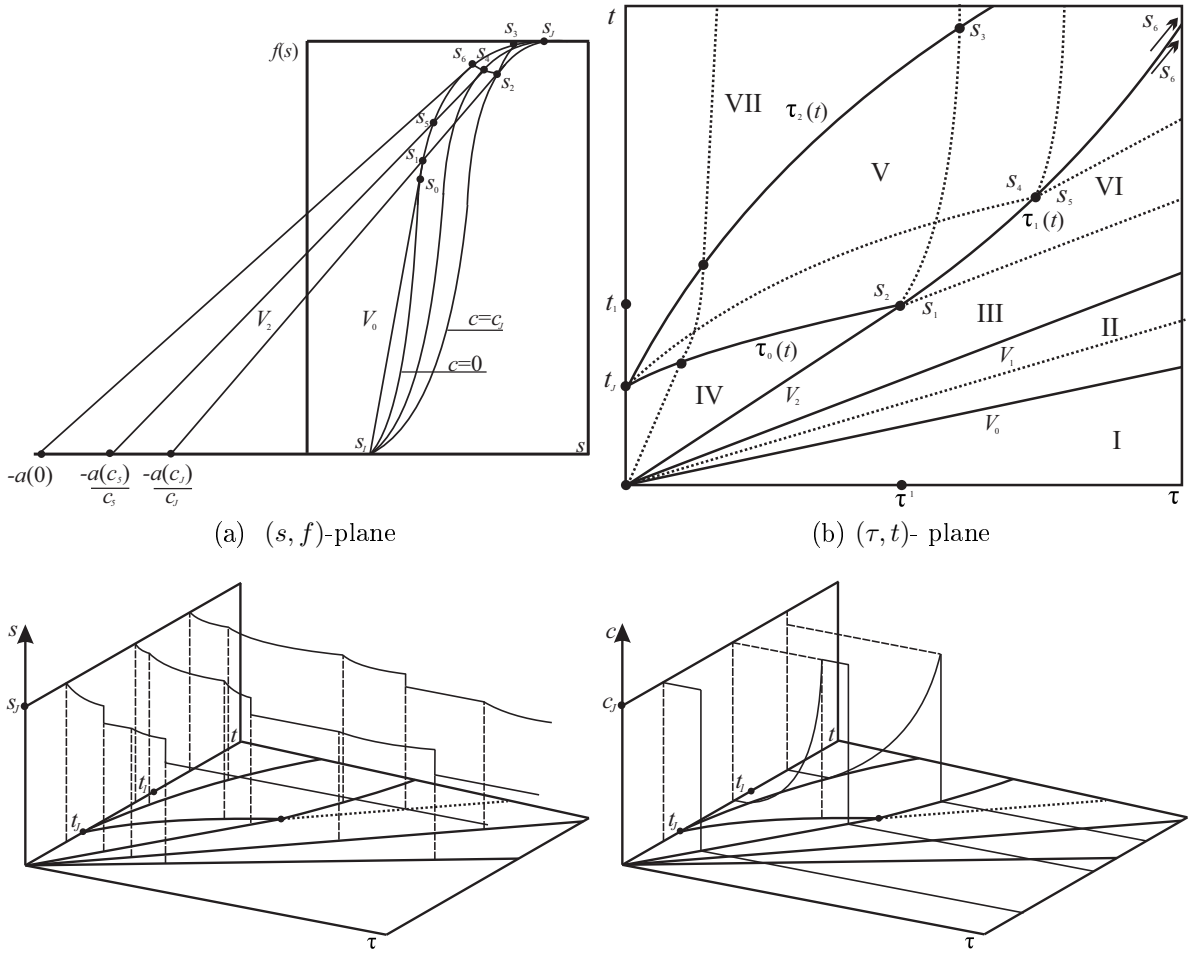

(a) (s, f)-plane (b) (τ, t)- plane

(c) Saturation - $s(\tau, t)$ (d) Concentration - $c(\tau, t)$

Figure 2: Solution of the 1-D problem, case 2

The solution is constructed using the hodograph transform in the regions where the interaction between rarefaction waves occurs. Thus, the path $s_J \to s_2 \to s_3 \to s_J$ in the (s, f)-plane transforms to $t_J \to s_2 \to s_3 \to t_J$ in the (τ, t)-plane. The velocity after the polymer slug is defined by the right-hand side of the equation

$$\frac{d\tau_2}{dt} = \frac{f(s(\tau_2), 0)}{s(\tau_2) + a'(0)}, \tag{3.2}$$

where τ_2 is the position of the rear part of the slug.

Fig.2 presents the solution of the problem in the case of the Langmuir isotherm. The structure of the solution can be divided into seven regions, see Table 2 for details.

4 Streamline Simulation Description. 2-D Case

The simulator is based on an IMPES formulation, in which the pressure field is calculated using an implicit finite-difference scheme. The water saturation and polymer con-

Region	Concentration	Saturation	Description
I.	$c(\tau,t)=0$	$s(\tau,t)=s_I$	Zone of displaced oil.
II.	$c(\tau,t)=0$	$s_0<s(\tau,t)<s_1$	The corresponding path in (s,f) plane is represented by part of a curve $f(s,0)$.
III.	$c(\tau,t)=0$	$s(\tau,t)=s_2$	Oil bank.
IV.	$c(\tau,t)=c_J$	$s^+(\tau_0)<s(\tau,t)<s_2$	Slug polymer. The corresponding path in (s,f) plane is represented by part of a curve $f(s,c_J)$.
V.	$0<c(\tau,t)<c_J$	$s^-(\tau_1)<s(\tau,t)<s^-(\tau_2)$	Slug polymer. The corresponding path in (s,f) plane is represented by part of a curve $f(s,c)$.
VI.	$c(\tau,t)=0$	$s_1<s(\tau,t)<s^+(\tau_1)$	The corresponding path in (s,f) plane is represented by a part of a curve $f(s,0)$.
VII.	$c(\tau,t)=0$	$s_J<s(\tau,t)<s^-(\tau_2)$	Water-drive zone. The corresponding path in (s,f) plane is represented by part of a curve $f(s,0)$.

Table 2: Structure of the 1-D problem, case 2

centration are calculated implicitly along the streamlines. The streamlines, launched from faces of a cell containing an injection well, are traced using Pollock's method [20]. The calculation procedure for streamline simulation is illustrated by the flowchart in Fig.3.

Equation (2.1) was discretized (Fig.4a) using the following finite-difference scheme:

$$T_{x_{i+1/2,j}}(P_{i+1,j}-P_{i,j})-T_{x_{i-1/2,j}}(P_{i,j}-P_{i-1,j})+ \\ +T_{y_{i,j+1/2}}(P_{i,j+1}-P_{i,j})-T_{y_{i,j-1/2}}(P_{i,j}-P_{i,j-1})=Q_{i,j}\,.$$

The transmissibility coefficients $T_{x_{i\pm1/2,j}}, T_{y_{i,j\pm1/2}}$ are calculated by:

$$T_{x_{i\pm1/2,j}}=\Big(\frac{k_xA_x}{\triangle x}(\lambda_o+\lambda_w)\Big)_{i\pm1/2,j}\,,$$
$$T_{y_{i,j\pm1/2}}=\Big(\frac{k_yA_y}{\triangle y}(\lambda_o+\lambda_w)\Big)_{i,j\pm1/2}\,,$$

where $A_x(A_y)$ is the cross-sectional area of the gridblock interface normal to the $x(y)$ direction and k_x, k_y are the components of the absolute permeability tensor $\mathbf{K}=\mathrm{diag}(k_x,k_y)$. Details of the solution of equation (3.2) and the determination of transmissibility on the faces of cells can be found in [19]. The total velocity of the fluid $\mathbf{u}=(u_x,u_y)$ is defined applying Darcy's law between two consecutive points of grid:

$$u_{x_{i\pm1/2,j}}=-\Big(\frac{k_x}{\triangle x}(\lambda_o+\lambda_w)\Big)_{i\pm1/2,j}(P_{i+1,j}-P_{i,j})\,,$$
$$u_{y_{i,j\pm1/2}}=-\Big(\frac{k_y}{\triangle y}(\lambda_o+\lambda_w)\Big)_{i,j\pm1/2}(P_{i,j+1}-P_{i,j})\,.$$

Considering a two-dimensional grid (Fig.4b), the total velocities within a cell in the x and y directions can be approximated by:

$$u_x=u_{x1}+\delta_x(x-x_1)\,,\ u_y=u_{y1}+\delta_y(y-y_1)\,,$$

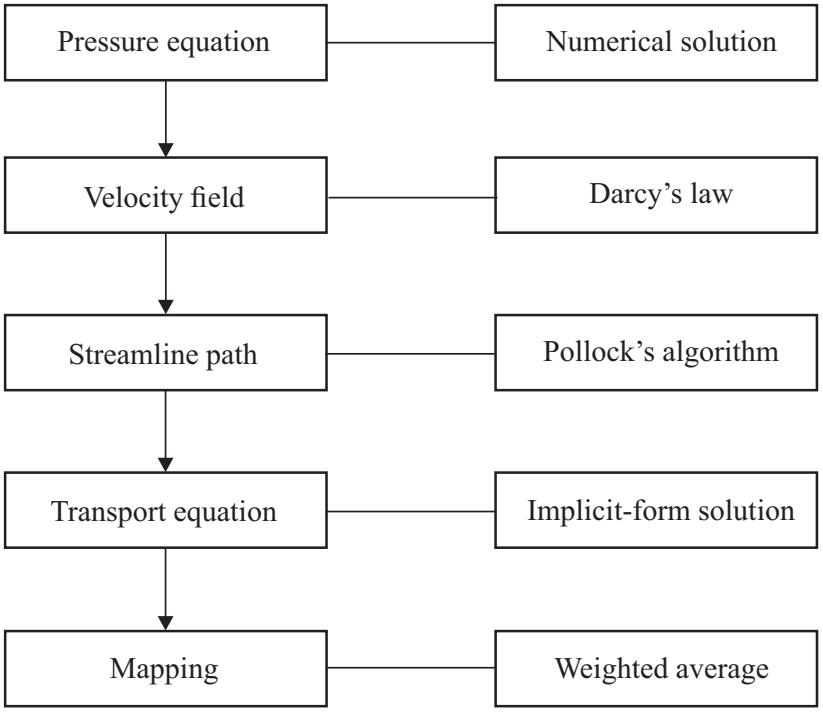

Figure 3: Major steps in streamline simulation

where δ_x and δ_y are the velocity gradients across the cell. The pathline and the time-of-flight can be calculated by integration of:

$$\frac{d\tau}{\phi} = \frac{dx}{u_x} = \frac{dy}{u_y}\,. \tag{4.1}$$

Assuming that the velocity changes linearly within the cell, equations (4.1) can be integrated from point (x_0, y_0) to an arbitrary point (x_i, y_i). The index $i = 1, 2$ indicates the face of the cell in each direction:

$$\begin{aligned}
\frac{\triangle\tau_{x_i}}{\phi} &= \int_{x_0}^{x_i} \frac{dx}{u_{x_0} + \delta_x(x - x_0)} = \frac{1}{\delta_x}\ln(\frac{u_{x_i}}{u_0})\,,\\
\frac{\triangle\tau_{y_i}}{\phi} &= \int_{y_0}^{y_i} \frac{dx}{u_{y_0} + \delta_y(y - y_0)} = \frac{1}{\delta_y}\ln(\frac{u_{y_i}}{u_0})\,.
\end{aligned}$$

Pollock's algorithm specifies that the proper exit face is the one that presents the lowest positive time-of-flight, calculated through:

$$\triangle\tau = \text{MinPositive}\{\triangle\tau_{x_1}, \triangle\tau_{x_2}, \triangle\tau_{y_1}, \triangle\tau_{y_2}\}\,.$$

The mapping of the saturation determined from the implicit-form solution along the streamlines to the finite-difference grid and calculation of the fractional flow of water in the producing well are performed using the approach proposed by Batycky [21]. The concentration of polymer in the production well is determined in a similar way. The

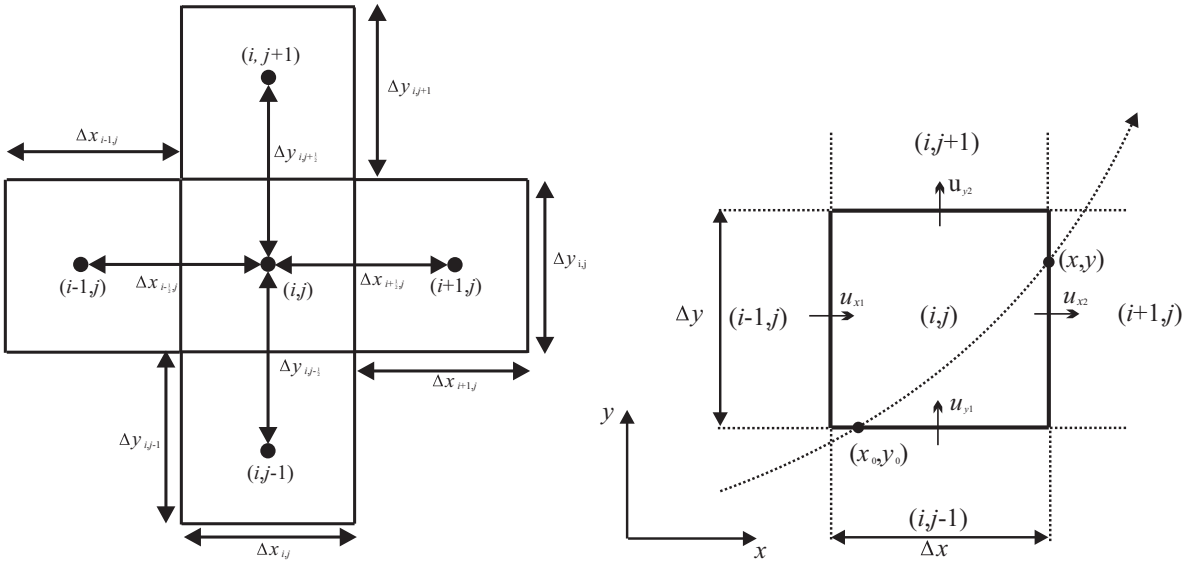

(a) Dimensions of a grid cell (b) Pathline within a cell

Figure 4: Simulation grid

saturation and concentration averages in a cell are calculated using a weighted average time-of-flight over the N streamlines crossing the cell:

$$\overline{s}_{cell} = \frac{\sum_{i=1}^{N} \triangle\tau_i \overline{s}_{sl}(t)_i}{\sum_{i=1}^{N} \triangle\tau_i} \, , \overline{c}_{cell} = \frac{\sum_{i=1}^{N} \triangle\tau_i \overline{c}_{sl}(t)_i}{\sum_{i=1}^{N} \triangle\tau_i} \, ,$$

where the saturation $\overline{s}_{sl}(t)_i$ and concentration $\overline{c}_{sl}(t)_i$ averaged over the streamline i are given by:

$$\overline{s}_{sl}(t)_i = \frac{1}{\triangle\tau_i} \int_{\tau_{ia}}^{\tau_{ib}} s(\tau,t)_i d\tau \, , \; \overline{c}_{sl}(t)_i = \frac{1}{\triangle\tau_i} \int_{\tau_{ia}}^{\tau_{ib}} c(\tau,t)_i d\tau \, .$$

5 Computational Results

In order to validate the accuracy of the streamlines simulator developed, the water-flooding of a 500m×500m 1/4 five-spot pattern reservoir was calculated using a 50×50 grid. The injection well rate was fixed (=30 m^3/day) and the flowing pressure of the producer was set constant (= 7000 kPa). For each adsorption isotherm (Figs.5a and 5b) both homogeneous ($k_x = k_y = 500$ mD) and heterogeneous reservoirs (Fig.5e) were analyzed. Relative permeability curves are calculated using the Corey relations:

$$k_{ro} = k_{rowi}\Big(\frac{1 - s - s_{or}}{1 - s_{wi} - s_{or}}\Big)^{n_o} \, , \; k_{rw} = k_{rwor}\Big(\frac{s - s_{wi}}{1 - s_{wi} - s_{or}}\Big)^{n_w} \, , \qquad (5.1)$$

where s_{or} is the residual oil saturation, s_{wi} is the irreducible water saturation, n_o and n_w are constants of the model, and k_{rowi} and k_{rwor} are the endpoints of the relative permeability curves for oil and water, respectively. The curves of fractional flow of water (Figs.5c and 5d) are constructed using (5.1).

Parameter	μ_R	μ_{wI}	μ_o	c_R	t_J	s_I	k_{rowi}	k_{rwor}	ϕ	s_{or}	s_{wi}	n_o	n_w
Value	5 (mPa.s)	0.5 (mPa.s)	8 (mPa.s)	0.4 (Kg/m³)	530 (day)	0.2	0.5	0.7	0.2	0.2	0.2	2	2

Table 3: Reservoir parameters

The relationship between the viscosity and concentration of the polymer slug is assumed to be linear

$$\mu_w(c) = \frac{\mu_R - \mu_{wI}}{c_R} + \mu_{wI}\,,$$

where μ_R is the reference viscosity of the polymer slug at the reference concentration c_R, and μ_{wI} is the viscosity of pure water. Table 3 presents other reservoir parameters.

The results obtained were compared to the commercial finite-difference simulator IMEX®, widely used in petroleum engineering. The linear adsorption isotherm and a polymer concentration of 0.1 kg/m^3 were used in the first simulation run. Figs.6 and 7 present the saturation and concentration maps, respectively. For the case of adsorption governed by this isotherm the commercial simulator results present dispersion in the vicinity of the polymer slug boundaries.

The saturation and concentration shocks are adequately captured by the streamlines simulation. Another important issue is the numerical diffusion increase with time seen in the finite-difference simulator. In Fig.6 the smearing of the slug front caused by numerical effects of the commercial software may also be verified.

Fig.8 compares the water fractional flow and the oil recovery factor for both simulators. The most important feature is the shock dissipation in the finite-difference results. In spite of these characteristics, both models are in good agreement, the maximum deviation between the recovery factors is about 4%.

Results for the heterogeneous case show a similar behavior (Figs.9 and 10). The streamlines simulator was able to capture the heterogeneity trends of the reservoir, while the commercial simulator numerical diffusion masked them. These differences in the saturation and concentration maps for the heterogeneous case are not so obvious when the water fractional flow and oil recovery factor are observed (Fig.11).

In the case of adsorption governed by Langmuir's isotherm the polymer injection concentration adopted was 0.4 kg/m^3. Again, the finite-difference method was not able to capture correctly the saturation and concentration shocks (Figs.12 and 13). The difference in the recovery factor was greater for this case, close to 8%. Maps of saturation and concentration present similar features as for the Henry isotherm, and will not be presented.

Another important advantage of the streamlines simulator over the conventional finite-difference model is the number of time steps necessary to obtain the pressure convergence (Table 4).

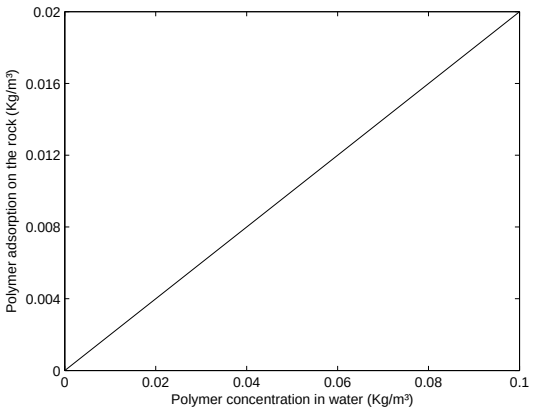

(a) Henry's isotherm

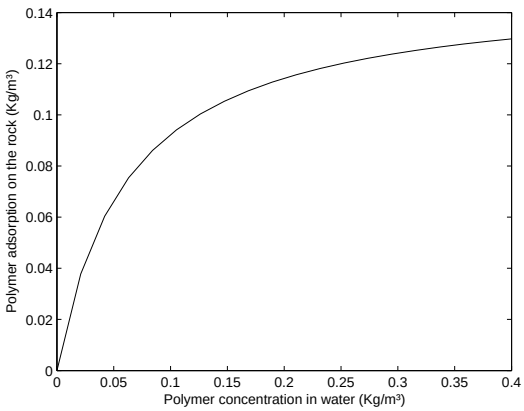

(b) Langmuir's isotherm

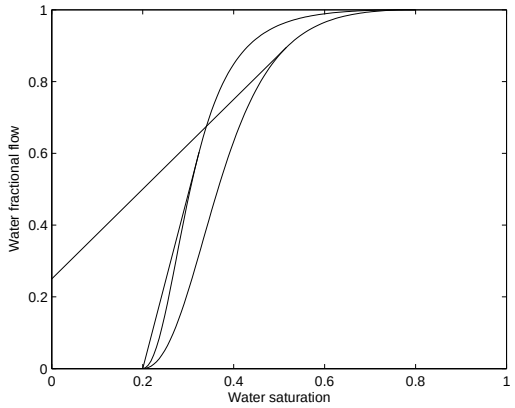

(c) Water fractional flow for Henry's isotherm

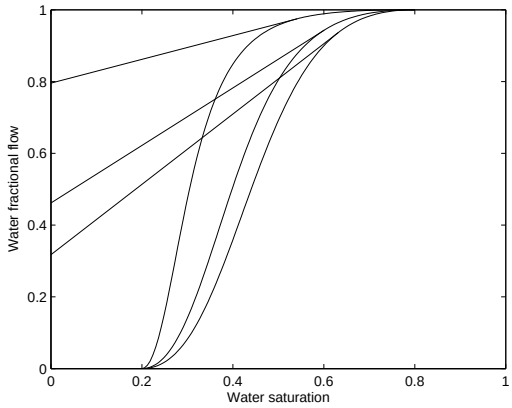

(d) Water fractional flow for Langmuir's isotherm

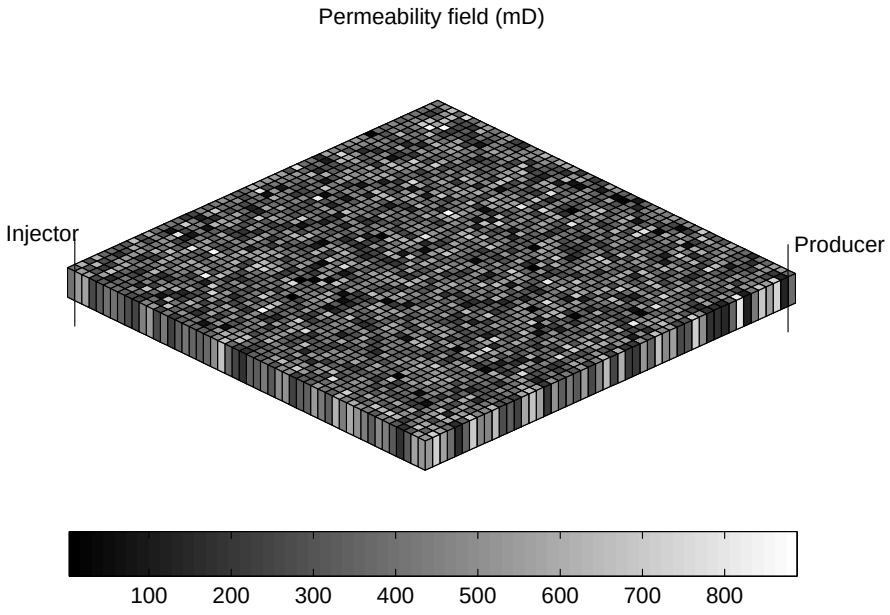

(e) Permeability field

Figure 5: Heterogeneous reservoir

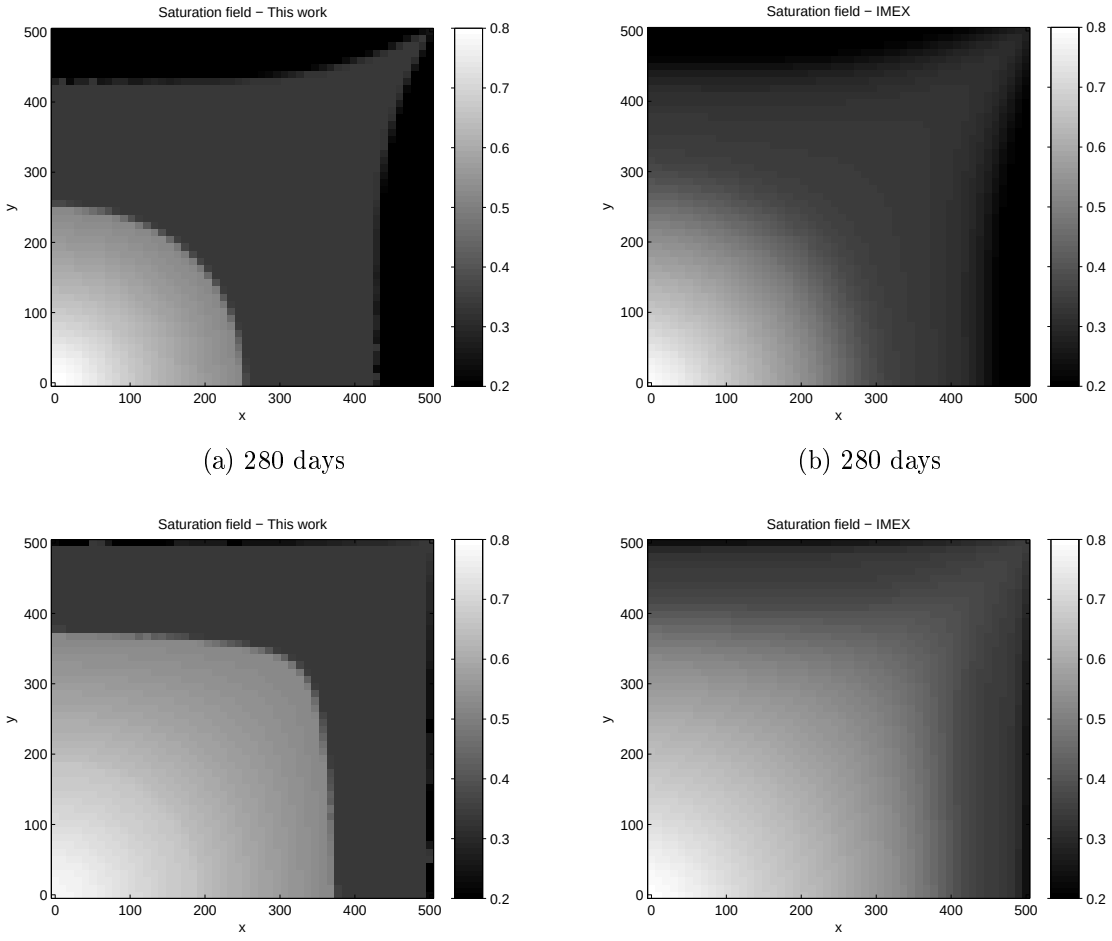

(a) 280 days

(b) 280 days

(c) 720 days

(d) 720 days

Figure 6: Saturation map. Case 1 - homogeneous model and Henry's adsorption isotherm

		This work	IMEX
Henry isotherm	Homogeneous case	50	254
	Heterogeneous case	50	263
Langmuir isotherm	Homogeneous case	50	206
	Heterogeneous case	50	299

Table 4: Number of time steps

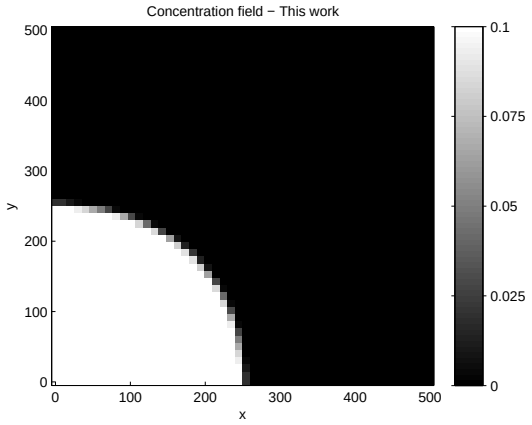

(a) 280 days

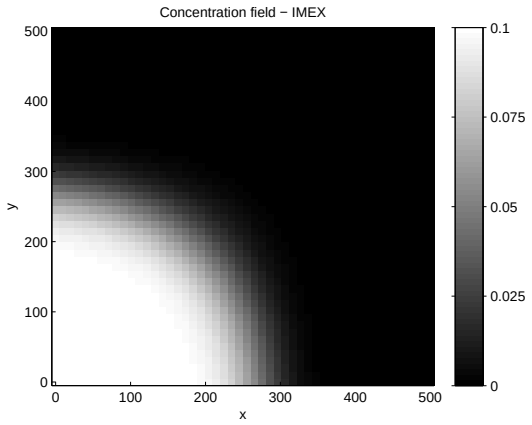

(b) 280 days

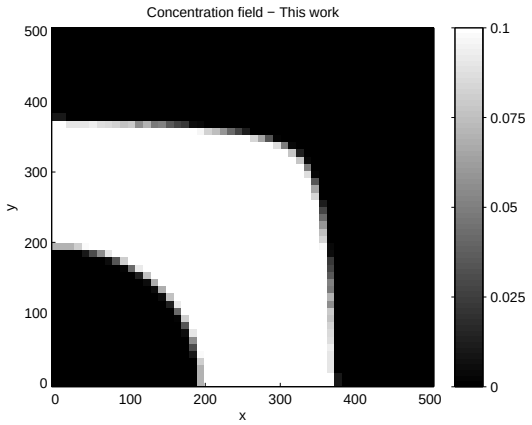

(c) 720 days

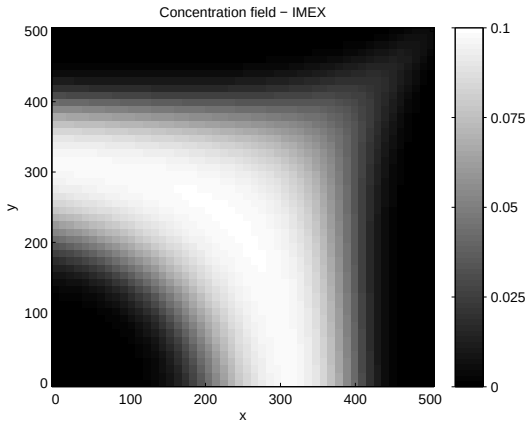

(d) 720 days

Figure 7: Concentration map. Case 1 - homogeneous model and Henry's adsorption isotherm

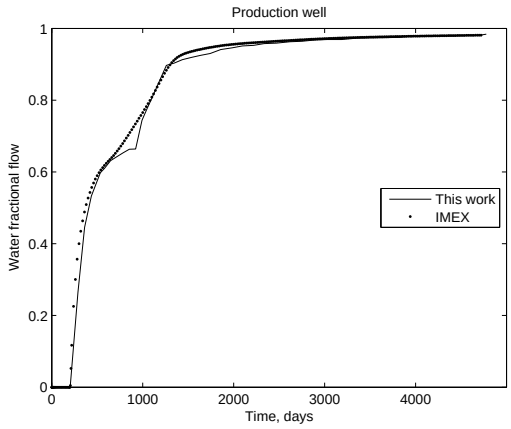

(a) Water fractional flow

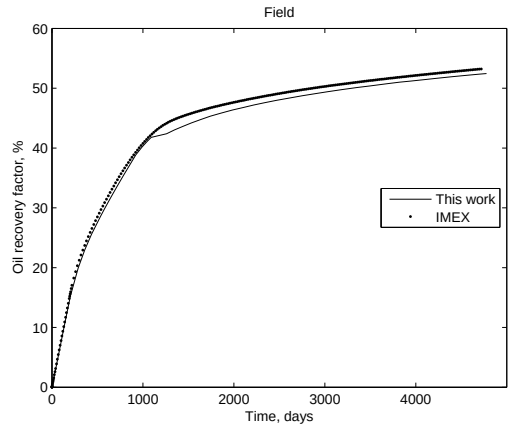

(b) Oil recovery factor

Figure 8: Case 1 - homogeneous model and Henry's adsorption isotherm

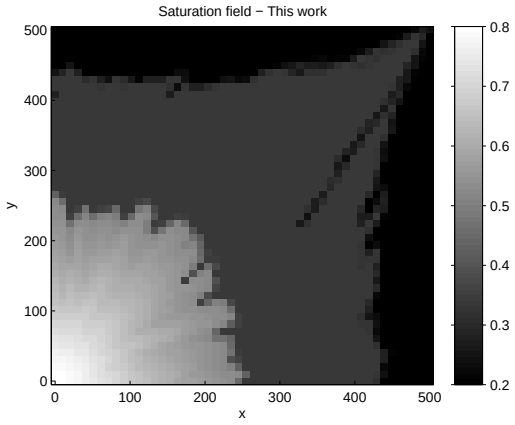

(a) 280 days

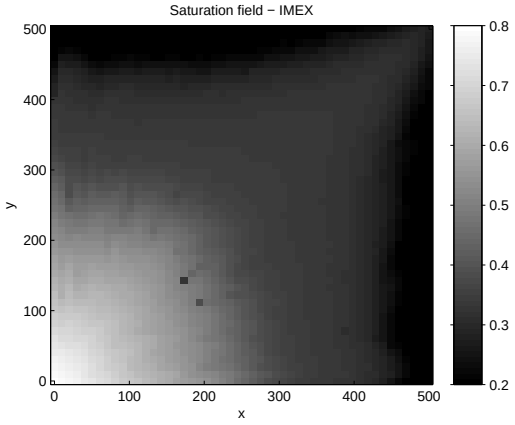

(b) 280 days

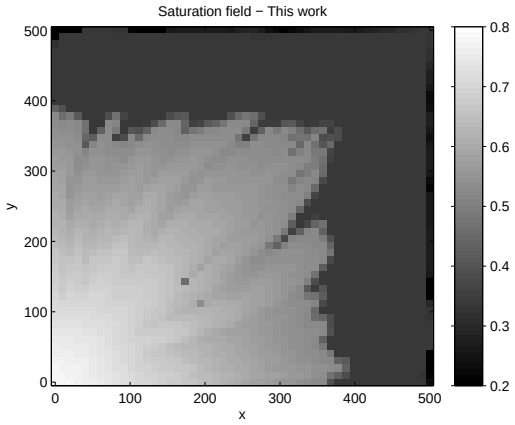

(c) 720 days

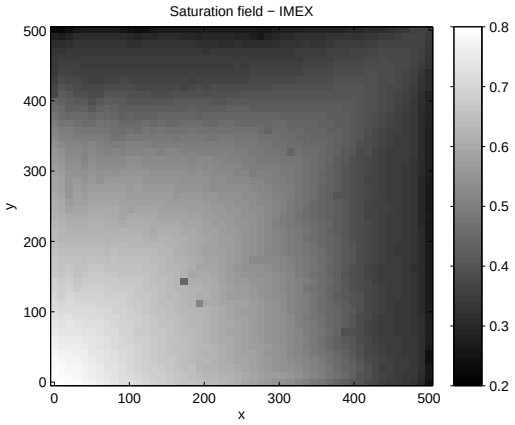

(d) 720 days

Figure 9: Saturation map. Case 1 - heterogeneous model and Henry's adsorption isotherm

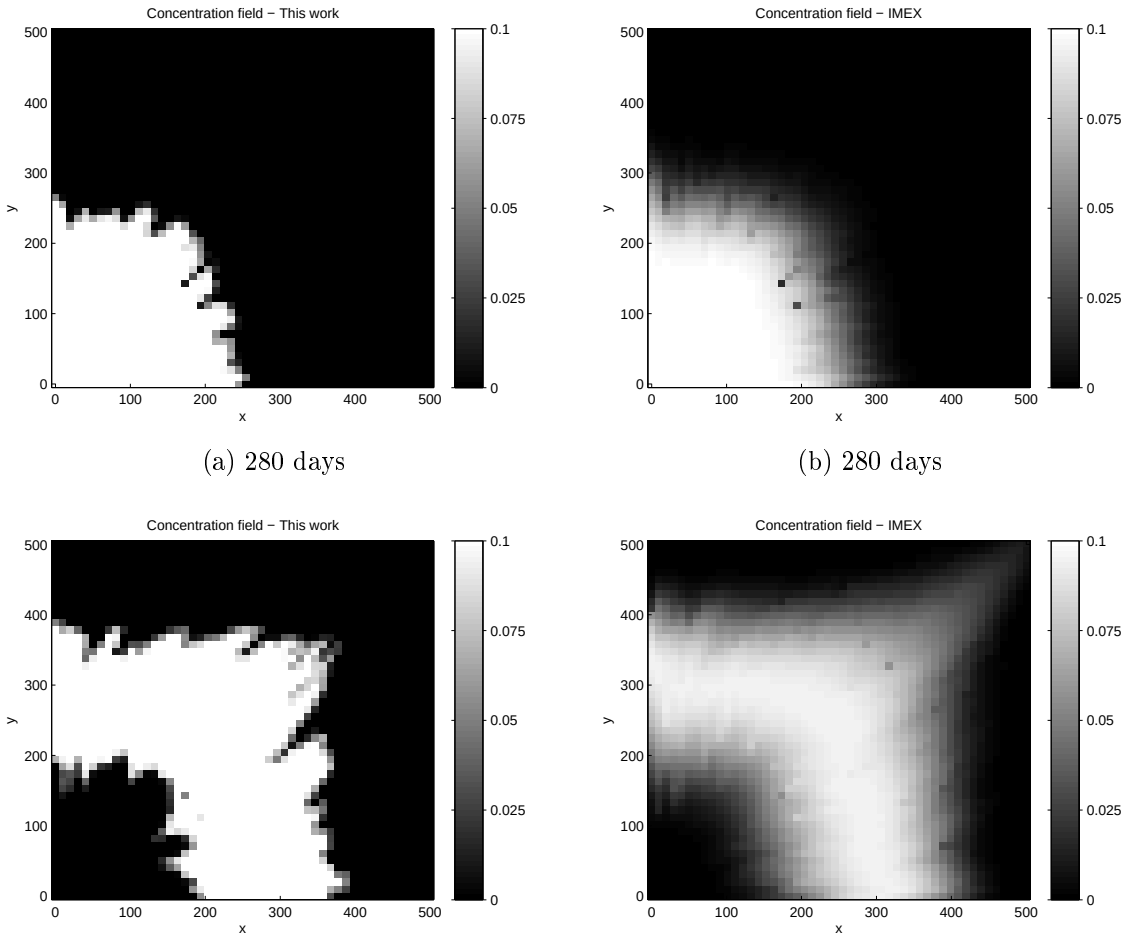

(a) 280 days

(b) 280 days

(c) 720 days

(d) 720 days

Figure 10: Concentration map. Case 1 - heterogeneous model and Henry's adsorption isotherm

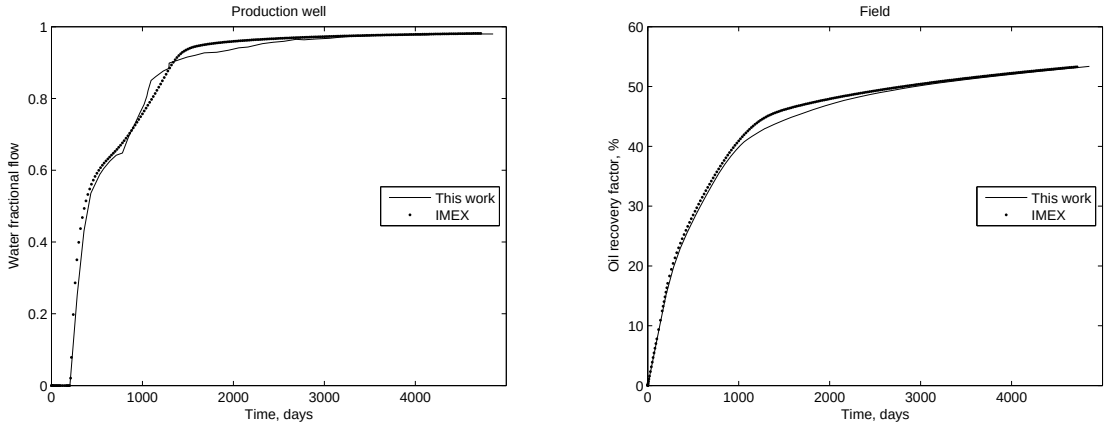

(a) Water fractional flow (b) Oil recovery factor

Figure 11: Case 1 - heterogeneous model and Henry's adsorption isotherm

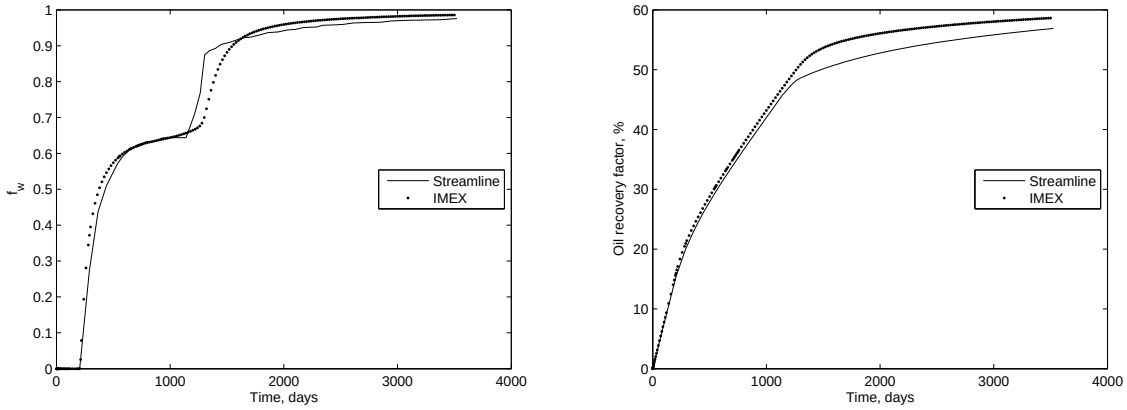

(a) Water fractional flow (b) Oil recovery factor

Figure 12: Case 2 - homogeneous model and Langmuir's adsorption isotherm

6 Conclusions

In this paper, a fast streamline method for a 2-D model describing the 2-phase oil displacement by polymer slugs considering adsorption effects was presented. The following conclusions can be derived:

1. A streamline simulator, capable to model the injection of polymer slugs where adsorption is governed by the Henry and Langmuir isotherms has been developed. The main feature of this simulator is the use of implicit-form solutions of the transport equations along the streamlines.

2. The results showed a good agreement compared to the commercial finite-difference simulator IMEX®, both in homogeneous and heterogeneous cases.

3. Streamlines simulation allowed a smaller number of pressure solvers and implicit-

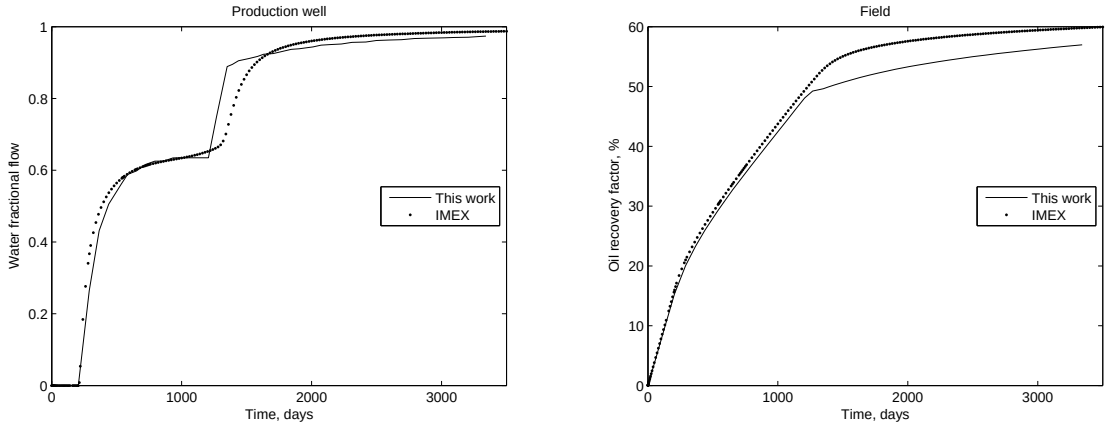

(a) Water fractional flow (b) Oil recovery factor

Figure 13: Case 2 - heterogeneous model and Langmuir's adsorption isotherm

form solutions have enabled a better estimative of the saturation and concentration shocks and rarefaction waves.

Acknowledgments

The authors wish to express their gratitude to the North Fluminense State University Darcy Ribeiro, Campos dos Goytacazes, Brazil for the technical and financial support for this study, and to the Macaé Section of SPE, Macaé, Brazil for sponsoring the Onepetro license. We would like also to thank an anonymous referee for helpful comments and suggestions.

Nomenclature

a = adsorption concentration of polymer on solid phase, ML^{-3}, $\mathrm{kg/m}^3$;
c = concentration of polymer solution, ML^{-3}, $\mathrm{kg/m}^3$;
$\overline{c}$ = average concentration, dimensionless ;
f = water fractional flow, dimensionless ;
f_s' = partial derivative of the water fractional flow with respect to saturation ;
$\mathbf{K}$ = absolute permeability tensor, L^2, mD ;
k_{ro} = oil phase relative permeability, dimensionless ;
k_{rowi} = oil relative permeability at irreducible water saturation ;
k_{rw} = water phase relative permeability, dimensionless ;
k_{rwor} = water relative permeability at residual oil saturation ;
n_o = oil Corey exponent, dimensionless ;
n_w = water Corey exponent, dimensionless ;
N = streamline number in a cell ;
P = pressure, $\mathrm{MT}^{-2}\mathrm{L}^{-1}$, kPa
q_J = injection rate, $\mathrm{L}^3\mathrm{T}^{-1}$, m^3/day ;
Q = injection/production total rate, $\mathrm{L}^3\mathrm{T}^{-1}$, m^3/day ;

s = water saturation, dimensionless ;
s_{or} = residual oil saturation, dimensionless ;
s_{wi} = irreducible water saturation, dimensionless ;
$\overline{s}$ = average saturation, dimensionless ;
t = time, days ;
$\mathbf{u}$ = total Darcy velocity, LT^{-1}, m/day ;
V_k = velocity of discontinuity k, dimensionless ;
Γ = Henry's isotherm constant, dimensionless ;
Γ_1 = Langmuir's isotherm constant, dimensionless ;
Γ_2 = Langmuir's isotherm constant, $\mathrm{L}^3\mathrm{M}^{-1}$, m^3/kg ;
$\triangle\tau_i$ = time-of-flight difference between the entry and exit in a cell for streamline i, T, days ;
λ = mobility, $\mathrm{L}^3\mathrm{TM}^{-1}$, mD/Pa.s ;
μ_o = oil viscosity, $\mathrm{ML}^{-1}\mathrm{T}^{-1}$, Pa.s ;
μ_R = reference viscosity, $\mathrm{ML}^{-1}\mathrm{T}^{-1}$, Pa.s ;
μ_w = polymer solution viscosity, $\mathrm{ML}^{-1}\mathrm{T}^{-1}$, Pa.s ;
μ_{wI} = pure water viscosity, $\mathrm{ML}^{-1}\mathrm{T}^{-1}$, Pa.s ;
ζ = coordinate along streamline, T, days ;
ξ = self-similar variable, dimensionless ;
τ = time-of-flight, T, days
τ_{ia} = time-of-flight of entry in a cell for streamline i, T, days ;
τ_{ib} = time-of-flight of exit in a cell for streamline i, T, days ;
τ_l = path of discontinuity l, T, days ;
ϕ = porosity, dimensionless ;
χ = streamfunction, L, m ;
ψ = streamfunction, $\mathrm{L}^2\mathrm{T}^{-1}$, m^2/day ;
Subscripts:
$cell$ = cell ;
I = initial ;
J = injection ;
o = oil ;
r = relative ;
R = reference ;
sl = streamline ;
w = water ;
Superscripts:
$+$ = value ahead of discontinuity ;
$-$ = value behind the discontinuity .

References

[1] W. Littmann, Enhanced Oil Recovery, Prentice Hall, 1980.

[2] K.S. Sorbie, Polymer-Improved Oil Recovery, Blackie, 1991.

[3] A. Datta-Gupta, K. N. Kulkarni, S. Yoon, D.W. Vasco, Streamlines, ray tracing and production tomography: generalization to compressible flow, Petroleum Geosciense, 7 (2001) S75-S86

[4] A. Datta-Gupta, M.J. King, A semianalytical approach to tracer flow modeling in heterogeneous permeable media, Advances in Water Resources, 18 (1995) 9-45.

[5] A. Datta-Gupta, M.J. King, Streamline Simulation: Theory and Practice, Vol.11, Richardson, Texas: Textbook Series SPE, 2007.

[6] L.W. Lake, J.R. Johnston, G.L. Stegemeier, Simulation and performance prediction of a large-scale surfactant/polymer project, SPE Journal 21(6) (1981) 731-739. SPE 7471-PA.

[7] R.P. Batycky, M.J. Blunt, M.R. Thiele, A 3D field-scale streamline-based reservoir simulator, SPE Reservoir Engineering 12(4) (1997) 246-254. SPE-36726-PA.

[8] M.R Thiele, R.P. Batycky, S. Pollitzer, T. Clemens, Polymer flood modeling using streamline-Part 1., Paper SPE 115545-MS presented at the SPE Annual Technical Conference and Exhibition, Denver, Colorado, 21-24 September of 2010. http://dx.doi.org/10.2118/16011-MS.

[9] T. Clemens, J. Abdev, M.R. Thiele, Improved polymer-flood management using streamlines, SPE Reservoir Evaluation & Engineering 14(2) (2011) 171-181. SPE-132774-PA.

[10] A.M. AlSofi, T.C. LaForce, M.J. Blunt, Sweep impairment due to polymers shear thinning, Paper SPE 120321-MS presented at the SPE Middle East Oil and Gas Show and Conference, Bahrain, 15-18 March of 2009.

[11] A.M AlSofi, M.J. Blunt, Streamline-based simulation of non-newtonian polymer flooding, SPE Journal 15(4) (2010) 895-905. SPE 123971-PA.

[12] F.J. Fayers, R.L. Perrine, Mathematical description of detergent flooding in oil reservoirs, Paper 1132-G presented at SPE Fall Meeting of the Society of Petroleum Engineers of AIME, Houston, Texas, 5-8 October of 1958. http://dx.doi.org/10.2118/1132-G.

[13] E.L. Claridge, P.L. Bondor, A graphical method for calculating linear displacement with mass transfer and continuously changing mobilities, SPE Journal 14(6) (1974) 609-618. SPE-4673.

[14] G.S.Braginskaya, V.M. Entov, Nonisothemal displacement of oil by a solution of an active additive, Fluid Dynamics 15(6) (1980) 873-880.

[15] T. Johansen, R. Winther, The Riemann solver for a two-phase multicomponent process, SIAM J. Math. Anal 20(4) (1989) 908-929.

[16] P.G. Bedrikovetsky, Displacement of oil by a slug of an active additive forced by water through a stratum, Fluid Dynamics, 17(3) (1982) 409-417.

[17] K.-H. Rhee, R. Aris, N.R. Amundson, First-Order Partial Equations, Vols. 1, 2, Englewood-Cliffs, New Jersey: Prentice-Hall, 1986.

[18] P.G. Bedrikovetsky, Mathematical Theory of Oil and Gas Recovery with Applications to ex-USSR Oil and Gas Fields, Kluwer Academic Press, 1993.

[19] T. Erterkin, J.H. About-Kassen, G.R. King, Basic Applied Reservoir Simulation, Richardson, Texas: Textbook Series SPE, 2001.

[20] D.W. Pollock, Semianalytical computation of path lines for finite-difference models, Ground Water 26(6) (1988) 743-750.

[21] R.P. Batycky, A Three-Dimensional Two-Phase Field Scale Streamline Simulator, PhD dissertation, Stanford University, Stanford, California (January 1997).

Bruno J. Vicente, Email: onurbjose@hotmail.com,
Adolfo P. Pires, Email: adolfo.puime@gmail.com,
Viatcheslav I. Priimenko, Email:slava211054@gmail.com,
Laboratory of Petroleum Engineering and Exploration,
North Fluminense State University Darcy Ribeiro
Rod. Amaral Peixoto, km163, Av. Brennand,
s/n, Imboassica, 27.925-535, Macaé, RJ, Brazil
Received 28 Mar 2013, in final form 23 Apr 2013